Japanese Journal of Applied Physics **53**, 071302 (2014) **REGULAR PAPER**
http://dx.doi.org/10.7567/JJAP.53.071302

Simultaneous observation of the diffusion of self-atoms and co-implanted boron and carbon in silicon investigated by isotope heterostructures

Masashi Uematsu*, Kota Matsubara, and Kohei M. Itoh

School of Fundamental Science and Technology, Keio University, Yokohama 223-8522, Japan
E-mail: uematsu@a3.keio.jp

Received March 14, 2014; accepted May 15, 2014; published online June 24, 2014

Diffusion of self-atoms and co-implanted carbon (C) and boron (B) in silicon (Si) has been simultaneously observed using $^{nat}Si/^{28}Si$ isotope heterostructures. The supersaturation of Si self-interstitials (I's) is investigated through the ^{30}Si diffusion. The experimental results showed that Si self-diffusion was enhanced, that is, the I is more severely supersaturated, while B diffusion near the kink region was reduced with higher C dose. We also found slower dissolution of immobile BI clusters. C diffusion was not significant, indicating the formation of immobile CI clusters. These results indicate that the reduction of B diffusion is not due to the trapping of I by C, if any, but due to the retardation of BI cluster dissolution by the presence of C to decrease the amount of mobile B. The Si self-diffusion is enhanced by the dissolution of CI clusters to emit I.

1. Introduction

Ultra-shallow junction formation is one of the most important issues in silicon (Si) device processing. During the post-implantation annealing, however, the transient enhanced diffusion (TED) by implantation-induced excess self-interstitials (I's) increases the junction depth.[1)] Co-implantation of carbon (C) in Si[2–11)] is a promising method to solve this issue because it is known to reduce boron (B) TED and is compatible with conventional device processing to only require limited device architecture change. C co-implantation reduces B TED in spite of the generation of its own additional damage by C implantation. One of the present authors proposed a model that implanted C atoms form immobile CI clusters with excess I induced by C implantation and that these CI clusters are stable and trap I to reduce B diffusion.[11)] However, the behavior of excess I has not yet been directly observed through Si self-diffusion in co-implantation of B and C. In this study, we simultaneously observed Si self-, B, and C diffusion using $^{nat}Si/^{28}Si$ isotope heterostructures that are co-implanted with B and C. We find that Si self-diffusion is enhanced with higher C dose, while B diffusion near the kink region (at B concentration of $4 \times 10^{18}\,cm^{-3}$) is reduced. The trapping of I by C cannot explain the experimental results because both Si self- and B diffusion occur via the I-mediated mechanism. We show that the B diffusion is reduced due to the retardation of BI cluster dissolution by the existence of C to decrease the amount of mobile B, while Si self-diffusion is enhanced by the dissolution of CI clusters to emit I.

2. Experiments

A ^{nat}Si (10 nm)/^{28}Si (10 nm) isotope heterostructure was grown by solid source molecular beam epitaxy.[12–14)] A high resistivity ($\rho > 2000\,\Omega\,cm$), 2 in., n-type, {001}-oriented floating zone ^{nat}Si (^{28}Si: 92.2%, ^{29}Si: 4.7%, and ^{30}Si: 3.1%) wafer was used as a substrate. A 100-nm-thick ^{nat}Si buffer layer was grown prior to the growth of the isotope heterostructures that is composed of the alternating layers of ^{nat}Si and isotopically pure ^{28}Si. C and B ions were implanted at room temperature into the isotope heterostructure samples at a tilt angle of 7°. The samples were first implanted with C at energy of 9 keV and with doses of 2×10^{14} or $1 \times 10^{15}\,cm^{-2}$. B was then implanted into both C preimplanted and unimplanted wafers at 7 keV and $2 \times 10^{14}\,cm^{-2}$. These implantation conditions were determined so that dopant concentration resembles that in actual device structures.[15)] After implantation, the wafers were cut into $5 \times 5\,mm^2$ squares for diffusion annealing. The samples were annealed in an inert gas atmosphere using a resistively heated furnace for 800 and 900 °C and a rapid thermal annealing apparatus for 1000 °C. The profiles of ^{30}Si, B, and C were measured by secondary ion mass spectrometry (SIMS). Primary ions used in SIMS were O_2^+ with the acceleration energy 2 keV for ^{30}Si and B, and Cs^+ with 3 keV for C.

3. Results

Figure 1 shows the depth profiles of ^{30}Si, B, and C in samples annealed at 900 °C for 30 min. The profiles of samples without C implantation and of those with 2×10^{14} and $1 \times 10^{15}\,cm^{-2}$ C are shown. ^{nat}Si layers have the natural abundance with 3.1% of ^{30}Si, whereas ^{28}Si layers are depleted of ^{30}Si. With such an implantation condition, the periodic depth profile of ^{30}Si is almost unperturbed after the implantation in comparison with the profile of ^{30}Si before the implantation. Therefore, an increase in surface roughness due to the implantation, which would deteriorate the periodic ^{30}Si SIMS profile, can be excluded. The actual interfaces between ^{nat}Si and ^{28}Si layers are abrupt (the degree of intermixing is only two atomic layers)[12–14)] and the smearing of the ^{nat}Si and ^{28}Si profiles is due to the SIMS artifact (knock-on mixing, etc.). The tail of the as-implanted B profile becomes slightly steeper with higher C dose because some B ions are dechanneled by C implant damage. Cross-sectional transmission electron microscopy images show that the samples remain single-crystalline even after the high-dose C implantation.

The ^{30}Si profiles in Fig. 1 showed that Si self-diffusion was enhanced with higher C dose and was significantly larger than the thermal equilibrium Si self-diffusion at 900 °C, which we have investigated using similar isotope heterostructures.[16)] The time-averaged enhancements of self-diffusion relative to the intrinsic thermal diffusion are 5 without C, 7 with $2 \times 10^{14}\,cm^{-2}$ C, and 12 with $1 \times 10^{15}\,cm^{-2}$ C. On the other hand, B diffusion near the kink region was reduced by the presence of C. For example, B diffusion lengths at the concentration of $4 \times 10^{18}\,cm^{-3}$ are 37 nm without C, 30 nm

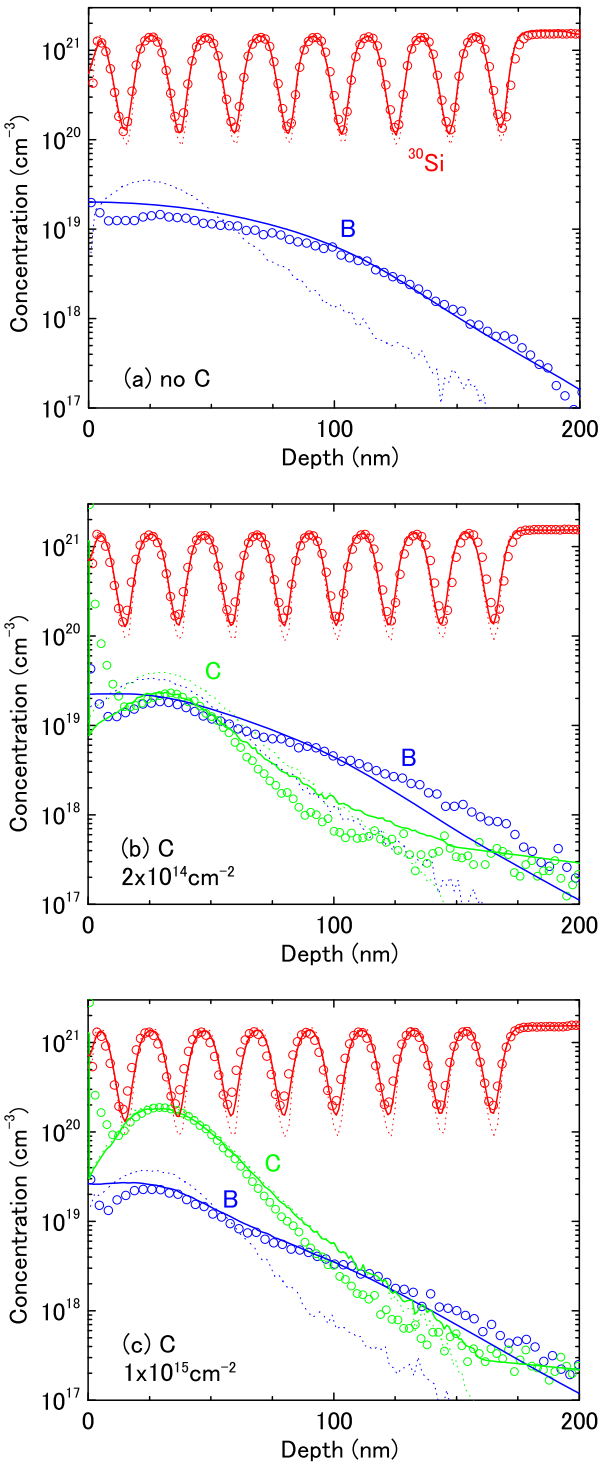

Fig. 1. (Color online) SIMS and simulated profiles of ^{30}Si, B, and C with 7 keV, 2×10^{14} cm^{-2} B implantation and annealing at 900 °C for 30 min. The profiles of samples (a) without C implantation and of those with (b) 2×10^{14} cm^{-2} and (c) 1×10^{15} cm^{-2} C implantation at 9 keV are shown. Broken lines and symbols represent the profiles of as-implanted and after annealing, respectively. Solid lines represent the simulation results.

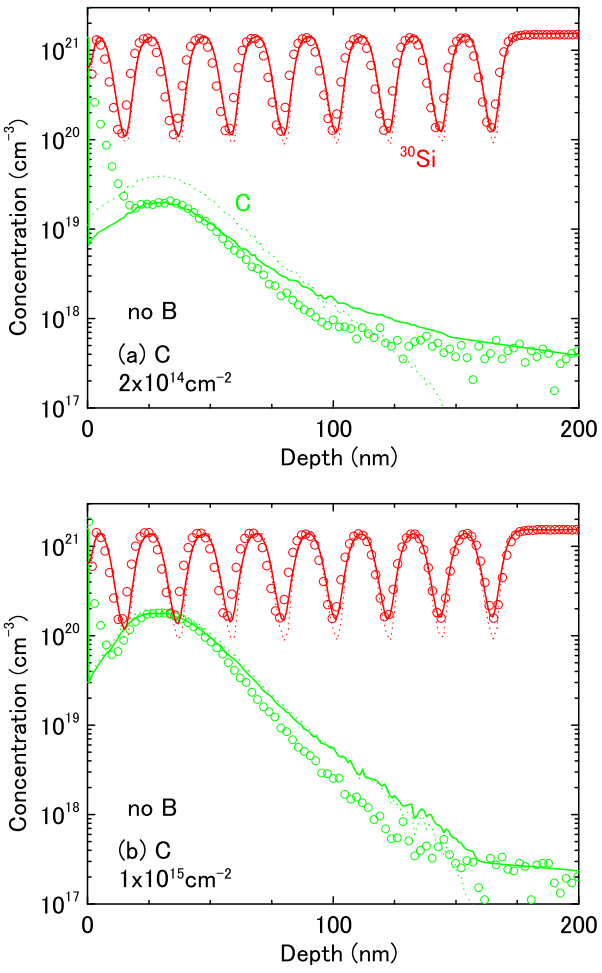

Fig. 2. (Color online) SIMS and simulated profiles of ^{30}Si and C without B implantation and with annealing at 900 °C for 30 min. The profiles of samples with (a) 2×10^{14} cm^{-2} and (b) 1×10^{15} cm^{-2} C implantation at 9 keV are shown. Broken lines and symbols represent the profiles of as-implanted and after annealing, respectively. Solid lines represent the simulation results.

with 2×10^{14} cm^{-2} C, and 22 nm with 1×10^{15} cm^{-2} C. In the B profiles, the demarcation between mobile and immobile B is seen at B concentration of $\sim 8 \times 10^{18}$ cm^{-3}. The immobile B is attributed to BI clusters, which are formed even at B concentrations far below the solubility limit under I supersaturation caused by ion implantation.[1,2,17] The B profiles showed that the amount of B in immobile BI clusters increases with higher C dose. This is attributable to slower BI cluster dissolution by the existence of C, leading to the decrease of the amount of mobile B.

The enhanced Si self-diffusion reveals that I supersaturation becomes higher with higher C dose. The contribution of vacancies (V's) to Si self-diffusion is negligibly small during TED because the I is supersaturated in over 10^4 (Refs. 18 and 19), as will be described below. In contrast, the reduction of B diffusion near the kink region was observed. This is particularly surprising in view of the fact that B diffusion is mediated by I. Assuming I trapping by C to decrease I concentration and hence to reduce B diffusion would contradict the enhanced Si self-diffusion. These results indicate that the reduction of B diffusion is not due to the trapping of I by C but due to the retardation of BI cluster dissolution by the existence of C to decrease the amount of mobile B. The contribution of I trapping by C, if any, is minor because Si-self diffusion is enhanced.

Figure 2 shows the depth profiles of ^{30}Si and C in samples implanted with only C, namely without B implantation, and annealed at 900 °C for 30 min. Even without B implantation, the Si self-diffusion is also enhanced with higher C dose. The time-averaged enhancements relative to the thermal diffusion

are 4 with $2 \times 10^{14}\,cm^{-2}$ and 8 with $1 \times 10^{15}\,cm^{-2}$ C. As also seen in Fig. 1, the C diffusion is not significant, although the I is supersaturated and C diffusion is mediated by I.[20] This can be explained by the model that all implanted C atoms form immobile CI clusters with excess I induced by C implantation.[11] Assuming the "+1 model"[21] for C implantation leads to the formation of C_nI_m clusters with $n \sim m$, which are different from mobile CI pairs. These results indicate that the CI clusters slowly dissolve to emit I and this is attributed to the enhanced Si self-diffusion. Note that the contribution of all the excess I generated by C implantation as free I would substantially overestimate the Si self-diffusion according to the diffusion simulation described below. B diffusion near the kink region is reduced; however, that at the tail region is rather enhanced, which is consistent with the enhanced Si diffusion. Actually, B diffusion lengths at the concentration of $1 \times 10^{18}\,cm^{-3}$ are 52 nm without C, 56 nm with $2 \times 10^{14}\,cm^{-2}$ C, and 59 nm with $1 \times 10^{15}\,cm^{-2}$ C. We suppose that C co-implantation is effective because junction depth near B kink regions may be important for device performance and as-implanted B profiles become steep due to dechanneling by C implant damage. The ^{30}Si profiles in Figs. 1 and 2 show that Si self-diffusion in co-implantation of B and C is larger than that in only C implantation with the same C doses. The I supersaturation in co-implantation of B and C originates from {311} I clusters, BI clusters, and CI clusters, while that in C only from CI clusters.

4. Discussion

In Figs. 1 and 2, we have observed enhanced Si-self diffusion, reduced B diffusion near the kink region, and slower dissolution of BI clusters with higher C dose in co-implantation of B and C at 900 °C. The same phenomena were also observed at other annealing temperatures of 800 and 1000 °C. These results lead us to conclude that the Si self-diffusion is enhanced by the dissolution of CI clusters to emit I and that the reduction of B diffusion is due to the retardation of BI cluster dissolution by the existence of C to decrease the amount of mobile B. In order to confirm this model, we performed a diffusion simulation of ^{30}Si, B, and C in the isotope heterostructures co-implanted with B and C. We used basically the same models and the same set of parameter values used in our previous study for co-implantation of B and C.[11] We simulated the diffusion based on our models for B diffusion,[22] C diffusion,[11] BI clusters[17] and CI clusters,[11] and that for {311} I clusters that takes Ostwald ripening into account,[18,19] as was done previously.[11,14,17] The changes made to take into account the models proposed in the present study are

(i) reducing dissolution rates of BI clusters, k_{dBIcl}, (k_{9d} in Ref. 11) by the presence of C,
(ii) alternating dissolution rates of I trapped in CI clusters, k_{dCIcl}, (k_{5d} in Ref. 11),
(iii) reducing trapping rates of I by CI clusters, k_{gCIcl}, (k_{3g} in Ref. 11) to zero, and
(iv) adding ^{30}Si diffusion via I and V in the same way as in Ref. 14 [Eqs. (4)–(6), (13)–(16), and (22)–(24)], including I–V recombination.

For the initial profile of {311} I clusters, the "+1" model[21] was used, as was done previously,[11] where the implanted profiles are multiplied by a factor of 1.0. In order to describe TED, we used the model of the time evolution of {311} I clusters during TED.[11,18,19] For the BI clustering model, we used the analytical formula [Eq. (5) in Ref. 17] to estimate the initial profiles, assuming that the BI clusters are formed at the very early stages of annealing. In addition, the initial profiles of BI clusters were estimated independent of the existence of C because the formation of BI clusters was not hindered by the presence of C.[11] For the dissolution of BI clusters, the origin of the retardation by the presence of C is not yet clear, as will be described below. Therefore, the k_{dBIcl} values are reduced to fit the experimental profiles. CI clusters are formed with an amount of I that equals the number of implanted C and the initial concentration of I trapped in CI clusters is determined by Eq. (3) in Ref. 11. Concerning the charge states of I, the contributions of neutral, singly, and doubly positive I (I^0, I^+, and I^{2+}) were taken into account, as was done previously,[14] because the I^{2+} contribution to self-diffusion is also important for p-type Si.[23] For the V contribution, neutral V, which is the dominant V state,[23] was taken into account and the V diffusivity in Ref. 16 was used. In addition, we used the diffusivities of B (Ref. 24) and C (Ref. 20) in thermal equilibrium conditions. Using the models and initial profiles mentioned above, diffusion equations were solved numerically by the partial differential equation solver ZOMBIE.[25]

Figures 1 and 2 show the simulated results for ^{30}Si, B, and C diffusion after annealing at 900 °C for 30 min. In addition, Fig. 3 represents the simulated and SIMS profiles for the C dose of $2 \times 10^{14}\,cm^{-2}$ at 800 °C for 30 min and for $1 \times 10^{15}\,cm^{-2}$ at 1000 °C for 5 s, where the time-averaged enhancements of self-diffusion relative to the thermal diffusion are 50 and 40, respectively. The SIMS profiles of ^{30}Si, B, and C were nicely fitted by the simulation and this indicates the validity of our model proposed in the present study. In the simulation, the parameter values of k_{dCIcl} were first determined with $k_{gCIcl} = 0$ from the fitting of ^{30}Si profiles without B implantation (see Fig. 2). The values determined are $k_{dCIcl} = 1 \times 10^{-4}$ and $3 \times 10^{-5}\,s^{-1}$ for 2×10^{14} and $1 \times 10^{15}\,cm^{-2}$ C, respectively, at 800 °C, 1×10^{-3} and $3 \times 10^{-4}\,s^{-1}$ at 900 °C, and 1×10^{-1} and $3 \times 10^{-2}\,s^{-1}$ at 1000 °C. The k_{dCIcl} values show a dependence on C dose, and those for $1 \times 10^{15}\,cm^{-2}$ C is systematically about one-third of those for $2 \times 10^{14}\,cm^{-2}$ C. CI clusters can have various compositions.[26] We suppose that lower C dose may leads to C_nI_m clusters with smaller numbers of n and m, which are less stable upon dissolution. Note that I diffusion is so fast that the depth profile of I concentration is almost flat except near the surface region,[14] and therefore, ^{30}Si profiles show no significant dependence on depth even though the supersaturated I's are originated from CI clusters. Then the values of k_{dBIcl} were determined. In order to fit the ^{30}Si and B profiles in the co-implantation, the k_{dBIcl} values previously used[11,14,17] were reduced by factors of 1 and 2 for 2×10^{14} and $1 \times 10^{15}\,cm^{-2}$ C, respectively, at 800 °C, by 7.5 and 15 at 900 °C, and by 2 and 4 at 1000 °C. The k_{dBIcl} values also show a dependence on C dose, and those for $1 \times 10^{15}\,cm^{-2}$ C is systematically one half of those for $2 \times 10^{14}\,cm^{-2}$ C. The dependence of k_{dBIcl} on C dose will be discussed below. We mention that the diffusion profiles of co-implanted C and B in our previous study[11] were also fitted by the present simulation using the modified parameters mentioned above.

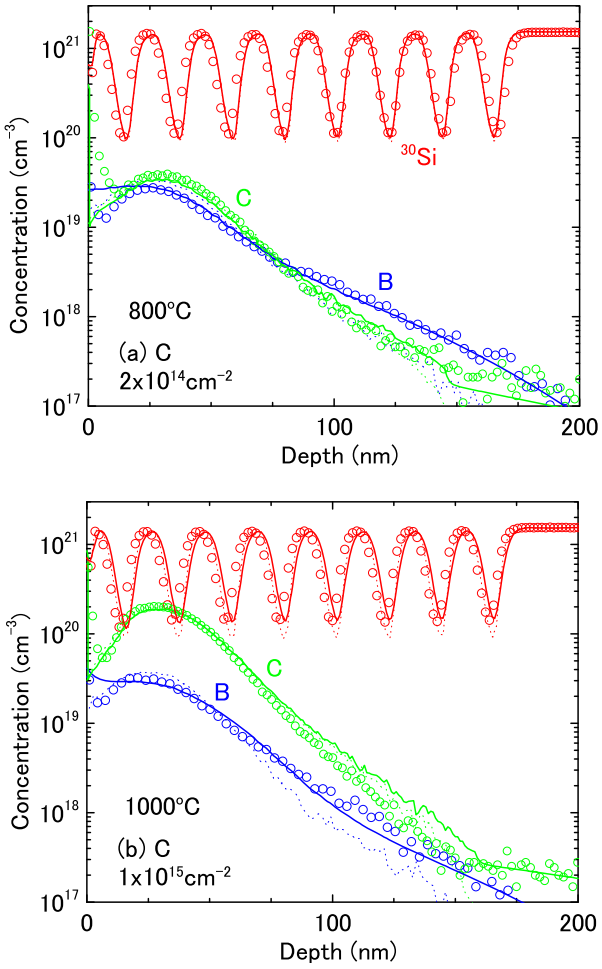

Fig. 3. (Color online) SIMS and simulated profiles of ^{30}Si, B, and C with 7 keV, 2×10^{14} cm^{-2} B implantation and with 9 keV C implantation. The profiles of samples with (a) 2×10^{14} cm^{-2} C implantation and annealing at 800 °C for 30 min and (b) 1×10^{15} cm^{-2} C implantation and annealing at 1000 °C for 5 s are shown. Broken lines and symbols represent the profiles of as-implanted and after annealing, respectively. Solid lines represent the simulation results.

The k_{dBIcl} value decreases with higher C dose, that is, the dissolution of BI clusters is retarded by the presence of C. The formation of C–B co-clusters, which have been recently observed,[10] is one possible cause of the retardation. C atoms in CI clusters, however, almost remain unmoved, while some B atoms in BI clusters are released during the annealing. This suggests that C atoms do not necessarily bond to B atoms. The temperature dependence of the reduction factor of k_{dBIcl} does not show a simple relation. We suggest that the dissolution of BI clusters is originally so slow that the retardation by C is minimal at 800 °C but is too fast to be effectively retarded at 1000 °C, although the origin of the retardation is not yet clear. While the presence of BCI clusters has been predicted,[27] further theoretical calculations are required to reveal the interaction between C, B and I. C diffusion was not significant; however, it was observed near the surface region and at the tail region, and was larger with smaller C dose and higher temperature, which is attributed to the dissolution of CI clusters.[11] This C decrease is more significant without B implantation than with it, as seen in Figs. 1 and 2. This seems to have the same origin as the retardation of BI cluster dissolution by the presence of C. For the dissolution rate of C trapped in CI clusters ($k_{4\mathrm{d}}$ in Ref. 11), the values used in the simulation for 900 °C are 3×10^{-4} and 4×10^{-4} s^{-1} with and without B implantation, respectively, for 2×10^{14} cm^{-2} C, and 5×10^{-5} and 6×10^{-5} s^{-1} for 1×10^{15} cm^{-2} C. The simulation results show that I undersaturation driven by the C diffusion[28] does not compensate the I supersaturation in TED because the supersaturation is much more severe than the undersaturation that would be expected from the C diffusion. The C decrease at the tail region is not satisfactorily fitted in the simulation probably because CI clusters with smaller C concentration are less stable upon dissolution; however, the C concentration is too small to affect the I supersaturation in TED. Therefore, the I undersaturation driven by the C diffusion, which would induce V supersaturation, cannot explain the enhanced Si self-diffusion. Mirabella et al. showed that substitutional C atoms in grown-in C layers trap I via the formation of immobile C_sC_i (substitutional and interstitial C) pairs.[29] In the present study, the concentration of substitutional C is so small (below 10^{18} cm^{-3}) due to the formation of CI clusters that the trapping of I by C is not significant. The present results suggest that B atoms are not necessarily a good marker to observe I supersaturation during TED because BI clusters can modulate B diffusion. Si isotopes are a more powerful tool for investigating the behaviors of I.

5. Conclusions

We have simultaneously observed Si self-, B, and C diffusion using $^{\mathrm{nat}}$Si/^{28}Si isotope heterostructures that are co-implanted with B and C. We found that Si self-diffusion was enhanced with higher C dose, which reveals more severe I supersaturation. On the other hand, B diffusion near the kink region was reduced and the dissolution of immobile BI clusters became slower with higher C dose. C diffusion was not significant, indicating the formation of immobile CI clusters. These results indicate that Si self-diffusion is enhanced by the dissolution of CI clusters to emit I, while the B diffusion is reduced due to the retardation of BI cluster dissolution by the presence of C to decrease the amount of mobile B.

Acknowledgments

We acknowledge Dr. Yasuo Shimizu of Tohoku University for the MBE growth. This work has been supported by Grants-in-Aid for Scientific Research No. 24560413 from the Japan Society for the Promotion of Science.

1) P. A. Stolk, H.-J. Gossmann, D. J. Eaglesham, D. C. Jacobson, C. S. Rafferty, G. H. Gilmer, M. Jaraiz, J. M. Poate, H. S. Luftman, and T. E. Haynes, J. Appl. Phys. **81**, 6031 (1997).
2) N. E. B. Cowern, A. Cacciato, J. S. Custer, F. W. Saris, and W. Vandervorst, Appl. Phys. Lett. **68**, 1150 (1996).
3) A. Vanderpool and M. Taylor, Nucl. Instrum. Methods Phys. Res., Sect. B **237**, 142 (2005).
4) B. J. Pawlak, T. Janssens, B. Brijs, W. Vandervorst, E. J. H. Collart, S. B. Felch, and N. E. B. Cowern, Appl. Phys. Lett. **89**, 062110 (2006).
5) E. J. H. Collart, S. B. Felch, B. J. Pawlak, P. P. Absil, S. Severi, T. Janssens, and W. Vandervorst, J. Vac. Sci. Technol. B **24**, 507 (2006).
6) M. Di Marino, E. Napolitani, M. Mastromatteo, G. Bisognin, D. De Salvador, A. Carnera, S. Mirabella, G. Impellizzeri, F. Priolo, H. Graoui, and M. A. Foad, Nucl. Instrum. Methods Phys. Res., Sect. B **253**, 46 (2006).
7) E. Augendre, B. J. Pawlak, S. Kubicek, T. Hoffmann, T. Chiarella, C. Kerner, S. Severi, A. Falepin, J. Ramos, A. De Keersgieter, P. Eyben, D.

Vanhaeren, W. Vandervorst, M. Jurczak, P. Absil, and S. Biesemans, Solid-State Electron. **51**, 1432 (2007).
8) C. H. Poon, A. See, Y. Tan, M. Zhou, and D. Gui, J. Appl. Phys. **103**, 084906 (2008).
9) T. Philippe, S. Duguay, D. Mathiot, and D. Blavette, J. Appl. Phys. **109**, 023501 (2011).
10) Y. Shimizu, H. Takamizawa, K. Inoue, T. Toyama, Y. Nagai, N. Okuda, M. Kato, H. Uchida, F. Yano, T. Tsunomura, A. Nishida, and T. Mogami, Appl. Phys. Lett. **98**, 232101 (2011).
11) M. Uematsu, J. Appl. Phys. **111**, 073517 (2012).
12) T. Kojima, R. Nebashi, K. M. Itoh, and Y. Shiraki, Appl. Phys. Lett. **83**, 2318 (2003).
13) Y. Shimizu and K. M. Itoh, Thin Solid Films **508**, 160 (2006).
14) Y. Shimizu, M. Uematsu, K. M. Itoh, A. Takano, K. Sawano, and Y. Shiraki, J. Appl. Phys. **105**, 013504 (2009).
15) A. Mineji and S. Shishiguchi, Ext. Abstr. Int. Workshop Junction Technology (IWJT '06), 2006, p. 84.
16) Y. Shimizu, M. Uematsu, and K. M. Itoh, Phys. Rev. Lett. **98**, 095901 (2007).
17) M. Uematsu, J. Appl. Phys. **84**, 4781 (1998).
18) M. Uematsu, Jpn. J. Appl. Phys. **36**, L982 (1997).
19) M. Uematsu, J. Appl. Phys. **83**, 120 (1998).
20) F. Rollert, N. A. Stolwijk, and H. Mehrer, Mater. Sci. Forum **38–41**, 753 (1989).
21) M. D. Giles, J. Electrochem. Soc. **138**, 1160 (1991).
22) M. Uematsu, J. Appl. Phys. **82**, 2228 (1997).
23) H. Bracht, H. H. Silvestri, I. D. Sharp, and E. E. Haller, Phys. Rev. B **75**, 035211 (2007).
24) M. Naganawa, Y. Kawamura, Y. Shimizu, M. Uematsu, K. M. Itoh, H. Ito, M. Nakamura, H. Ishikawa, and Y. Ohji, Jpn. J. Appl. Phys. **47**, 6205 (2008).
25) W. Jüngling, P. Pichler, S. Selberherr, E. Guerrero, and H. W. Pötzl, IEEE Trans. Electron Devices **32**, 156 (1985).
26) R. Pinacho, P. Castrillo, M. Jaraiz, I. Martin-Bragado, J. Barbolla, H.-J. Gossmann, G.-H. Gilmer, and J.-L. Benton, J. Appl. Phys. **92**, 1582 (2002).
27) C.-L. Liu, W. Windl, L. Borucki, S. Lu, and X.-Y. Liu, Appl. Phys. Lett. **80**, 52 (2002).
28) H. Rücker, B. Heinemann, W. Röpke, R. Kurps, D. Krüger, G. Lippert, and H. J. Osten, Appl. Phys. Lett. **73**, 1682 (1998).
29) S. Mirabella, A. Coati, D. De Salvador, E. Napolitani, A. Mattoni, G. Bisognin, M. Berti, A. Carnera, A. V. Drigo, S. Scalese, S. Pulvirenti, A. Terrasi, and F. Priolo, Phys. Rev. B **65**, 045209 (2002).